Contents lists available at ScienceDirect

Arabian Journal of Chemistry

journal homepage: www.ksu.edu.sa

Original article

Can MWCNT (20%)-MgO (80%)/10W40 nano-lubricant be used in industries? (Statistical analysis by focusing on economic factors and rheological behavior for best lubrication conditions)

Mohammad Hemmat Esfe [a], Hossein Hatami [b], Soheyl Alidoust [a,c], Davood Toghraie [d,*]

[a] Nanofluid Advanced Research Team, Tehran, Iran
[b] Associate Professor, Department of Mechanical Engineering, Lorestan University, Khorramabad, Iran
[c] School of chemistry, Damghan university, Damghan, Iran
[d] Department of Mechanical Engineering, Khomeinishahr Branch, Islamic Azad University, Khomeinishahr, Iran

ARTICLE INFO

Keywords:
Viscosity
MgO
MWCNTs
nanofluid
Hybrid nanofluid
experimental
statistical
correlation
margin of deviation

ABSTRACT

Hybrid nanofluid (NF) is a new generation of NF that create different and sometimes desirable properties due to the combination of two or more nanoparticles (NPs). Also, they have higher physical properties than conventional NFs in terms of thermal conductivity (TC) and viscosity. In this study, the rheological behavior of MWCNT-MgO (20:80)/10 W40 hybrid NF using 174 experimental data in temperature conditions T = 5–55 °C, solid volume fractions SVF = 0.05–1% and the shear rate SR = 666.5–11997 s^{-1} was investigated. The results of the experiments show that increasing the temperature reduces the viscosity of the BF. It is observed that temperature changes have the greatest effect on the viscosity of NFs. To predict the viscosity of hybrid NF, an empirical relationship based on temperature, SVF, and SR parameters is proposed. Comparing the price-performance ratio of different hybrid NFs concerning price performance factor (PPF), the results of this comparison show that the relative viscosity may be higher than other NFs, but its PPF is lower. To fit the curve of this relationship, the step-by-step regression method with a determination coefficient of 0.9973 is used. The experimental data have an acceptable agreement with the predicted data.

1. Introduction

NF is obtained by suspending metal particles or metal oxide with a diameter of less than 100 nm in normal fluids such as oil and water. Today, the use of nanotechnology has found a high position in responding to problems and meeting human needs (Alizadeh et al., 2023; Dai et al., 2023; Ruhani et al., 2022). One of the important characteristics of fluids that makes them important for various applications is their thermal conductivity of fluids, but it should be noted that the rheological properties of fluids are also very important due to their influence on pressure drop and pumping power. For this reason, most of the researchers' research is on investigating the rheological properties of different fluids (Wu et al., 2021; Wangjian et al., 2021). One of the dimensions of using this technology is the use of nano in fluids to achieve better properties (Tian et al., 2021; Mousavi et al., 2021; Banisharif et al., 2021; Keykhosravi et al., 2021). The addition of solid NPs into BFs improves the TC of BFs (Saboori et al., 2017; Hosseinian Naeini et al., 2016) and viscosity, which is very important in various industries. Fig. 1 schematically shows how to prepare NF. The addition of very small solids significantly improves the thermal properties of BFs.

NPs have created extensive applications for nanotechnology, which is generally known as science and research in the field of advanced materials. When the equipment made based on nanotechnology replaces the conventional equipment, the mechanisms are changed and sometimes several completely new functions are expected regarding the product. Also, many of the compounds that are presented with nanotechnology show very favorable characteristics, which are unique in turn. Evidence shows that a very high percentage of future products will rely on nanotechnology (Zhang et al., 2021). This technology can greatly improve the quality of human life (Guzman et al., 2006; Binu et al., 2014). In recent years, due to the increase of human capacity in the production of NPs, much attention has been paid to this type of material. Today, NPs are used in various industries such as the electronics industry, medical applications, pharmaceuticals, automotive industry, and environmental processes. Due to the significant potential of this

* Corresponding author.
E-mail address: Toghraee@iaukhsh.ac.ir (D. Toghraie).

https://doi.org/10.1016/j.arabjc.2023.105469
Received 3 September 2022; Accepted 18 November 2023
Available online 22 November 2023

Nomenclature

ρ	density
n	Power-law index
T	Temperature
$\dot{\gamma}$	Shear rate
τ	shear stress
m	consistency index
μ_r	Relative viscosity
w	Weight percent
μ_{nf}	Dynamic viscosity of the NF
μ_{bf}	Dynamic viscosity of the BF
φ	Solid volume fraction
MOD	margin of deviation
TC	Thermal conductivity
APS	Average particle size
MWCNT	Multi-walled carbon nanotube
RSM	Response surface methodology
SEM	Scanning Electron Microscope
TEM	Transmission electron microscope
XRD	X-Ray diffraction

technology, investment in the field of nanotechnology applications is growing worldwide (Valantina et al., 2018). The rheological behavior of NFs and their convective properties are used in heat transfer processes. Some applications of NFs in different equipment are shown in Fig. 2.

TC (Ehteram et al., 2016; Hosseinian Naeini et al., 2016; Raei et al., 2016; Abbasian Arani et al., 2016; Eshaghi and Mojab, 2017; Fuxi et al., 2021; Jamei et al., 2021; Yang et al., 2021) and viscosity (Makinde and Mishra, 2017; Dezfulizadeh et al., 2021; Hosseini and Dehaj, 2021; Shahsavar et al., 2021) are the most important properties of fluids in industrial heat transfer processes. Despite the efforts of researchers to provide a precise relationship to determine the TC and viscosity of NFs, no general and unified relationship was established to determine the thermophysical properties of NFs. Also, the presented relations depending on the type of BF, SVF, and temperature show different results. Table 1 presents some of the presented relations regarding the viscosity of the NFs.

As mentioned, viscosity is one of the characteristics of NFs. So far, many measures have been taken in this field of viscosity and various scientific reports have been published. In this section, some related works to viscosity are mentioned (Yu et al., 2021; Ghanbari and Rezazadeh, 2021; Cao et al., 2021; Mousavi et al., 2021; Hosseini and Dehaj, 2021; Sun et al., 2021). Esfe et al., are leading researchers in the development of hybrid NFs (Esfe et al., 2015, 2017; Esfe and Sarlak, 2017; Hemmat Esfe et al., 2015). Abdullahi et al. (Moghaddam and Motahari, 2017) reported the changes in rheological behavior and lubrication of the hybrid composition of CuO with MWCNTs NPs in SAE40 engine oil. The findings show that the viscosity of the hybrid NF was 29.47 % higher than the viscosity of BF at SVF of 1%. Alidoust et al. (Alidoust et al., 2022) investigated the thermal conductivity of hybrid NF containing SWCNTs and Fe_3O_4 at different SVFs and temperatures. Esfe et al. (Esfe et al., 2021) analyzed the dynamic viscosity of MWCNT-TiO_2 (50:50)/5W50 engine oil NF at T = 5–55 °C and SVF = 0.05 % −1%. The results indicate that the NF is non-Newtonian. Alirezaie et al. (Alirezaie et al., 2017) evaluated the rheological behavior of oil-based hybrid NFs at different SVFs, temperatures, and SRs. To perform this test, six different SVFs with percentages of 0.0625, 0.125, 0.25, 0.5, 0.75 and 1 % at T = 25, 30, 35, 40, 45 and 50 °C and six SRs from 670 to 870 s^{-1} were considered. The results show that the dynamic viscosity of NFs decreases drastically with increasing temperature. As a result, increasing the SVF increases the viscosity. Nadooshan et al. (Nadooshan et al., 2017) investigated the dynamic viscosity of 10 W40 lubricant containing hybrid NPs of 90 % silica (SiO_2) and 10 % MWCNTs. NF samples were prepared by a two-step method with SVF = 0.05, 0.1, 0.25, 0.5, 0.75 and 1 %. The dynamic viscosity of the samples was measured at T = 5 and 55 °C and SR = 666.5 s^{-1} to 11997 s^{-1}. Experimental results show that NFs behave non-Newtonian at all temperatures, while oil 10 W40 behaves non-Newtonian only at high temperatures. In this study, the dynamic viscosity of MWCNT (20 %)-MgO (80 %)/10 W40 HNF has been investigated experimentally and statistically. In the laboratory study, the effect of temperature, SVF, and SR on μ_{nf} will be investigated. The approach of this article is to present a comprehensive report of the comparison of NPs with different percentages in engine oil against the performance in different environmental conditions by analyzing the viscosity of NFs. The purpose of this research is to create suitable viscosity for engine operation in different weather conditions by adding suitable NPs to engine oil. Engine oil with these characteristics will increase the quality and efficiency as well as the engine's lifespan and prevent possible damages. It affects the moving parts of the car due to friction and wear. In the final part, to improve the quality and efficiency of nanoparticles and the durability of parts and reduce costs, the MOD method was used to compare the viscosity of experimental results with obtained results from the proposed equation.

2. Experimentation

2.1. NF preparation

In this research, NFs were prepared with a common two-step method

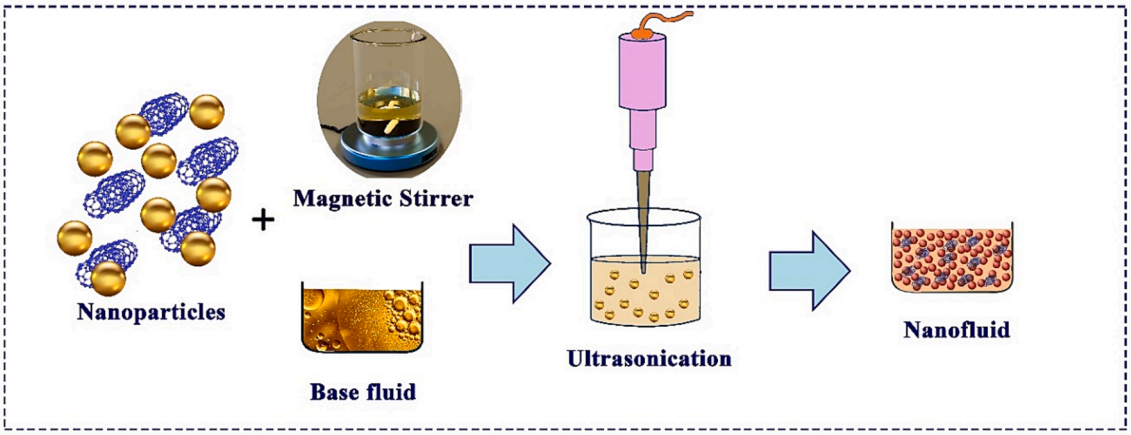

Fig. 1. Schematic of NF preparation.

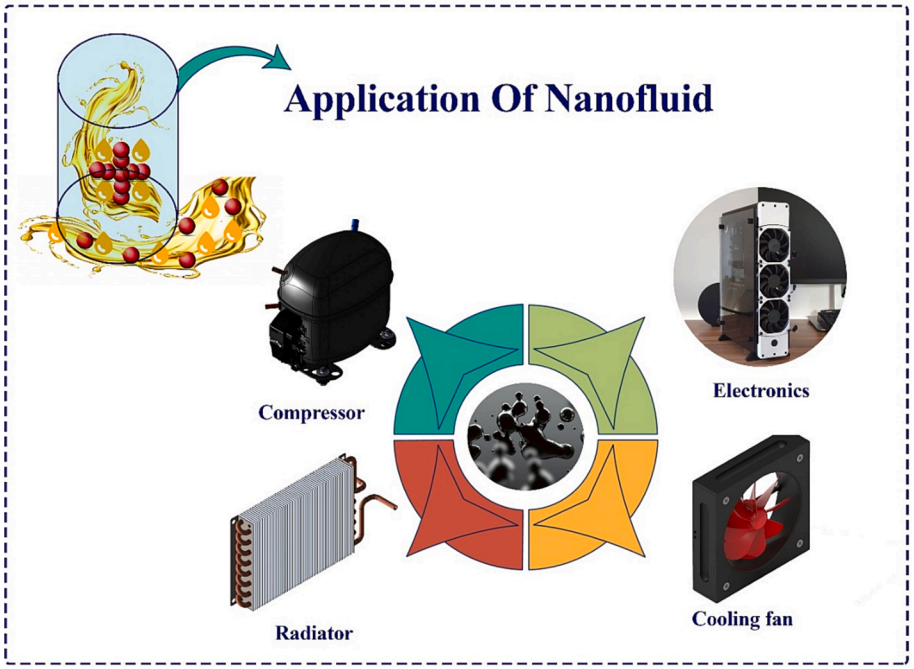

Fig. 2. Applications of NFs in different equipment.

Table 1
Examples of experimental relations of dynamic viscosity of NFs.

year	Eq.	Ref.
1906	$\mu_{nf} = (1+2.5\varphi)\mu_{bf}$	(Einstein, 1906)
1951	$\mu_{nf} = exp\left(\frac{2.5\varphi}{1-\frac{\varphi}{\varphi_m}}\right)\mu_{bf}$ $1.35 < k < 1.91$ $0.523<\varphi_m < 0.740$	(Mooney, 1951)
1952	$\mu_{nf} = \left(\frac{1}{(1-\varphi)^{2.5}}\right)\mu_{bf}$	(Brinkman, 1952)
1959	$\mu_{nf} = \left[1-\frac{\varphi_p}{\varphi_m}\right]\mu_{bf}\varphi_m = 0.64$	(Krieger and Dougherty, 1959)
1967	$\mu_{nf} = \frac{9}{8}\left(\frac{(\varphi/\varphi_m)^{1/3}}{1-\left(\frac{\varphi}{\varphi_m}\right)^{1/3}}\right)\mu_{bf} 0.523<\varphi_m < 0.740$	(Frankel and Acrivos, 1967)
2003	$\mu_{nf} = (0.4513e^{0.6965\varphi})\mu_{bf}$	(Tseng and Chen, 2003)
2007	$\mu_{nf} = \left(1+10.6\varphi+(10.6\varphi)^2\right)\mu_{bf}$	(Chen et al., 2007)
2009	$\mu_{nf} = (A+B\varphi+C\varphi^2)\mu_{bf}$	(Duangthongsuk and Wongwises, 2009)
2010	$\mu_{nf} = (1.005+.497\varphi-0.1149\varphi^2)\mu_{bf}$	(Godson et al., 2010)
2010	$\mu_{nf} = \left[\frac{1}{1-2.5\varphi}\right]\mu_{bf}$	(Abedian and Kachanov, 2010)
2016	$\mu_{nf} = \left(1.089+\left[-7.722\times10^{-9}\left(\frac{T}{\varphi}\right)^2+1.1917T^{0.298}\varphi^{0.4777}\right]\times exp\left(19457T^{-0.453}\varphi^{3.219}\right)\right)\mu_{bf}$	(Baratpour et al., 2016)

(Fig. 3). The first part of preparing NFs is to disperse the NPs in the BF and then stabilize the suspension. In this work, additive NPs consisting of MWCNT and MgO with a combined ratio of 20 %: 80 % were used in 10 W40 BF (See Fig. 3).

Methods of analysis and identification of materials are very important because the physical and chemical properties of a product depend on the type of raw materials and their microstructure. Therefore, identification methods and equipment are needed to identify the microstructure of each material and, as a result, the properties of that material to conduct research and quality control of industrial products. Advanced TEM and XRD imaging methods are special tools in determining the structure and morphology of materials (size, shape), which allow studying the microstructure of materials with high resolution and very high magnification. According to Figs. 4 and 5, the average diameter of the magnesium oxide NPs is about 50 nm, the diameter, the inner and outer diameters of the MWCNTs are of good quality.

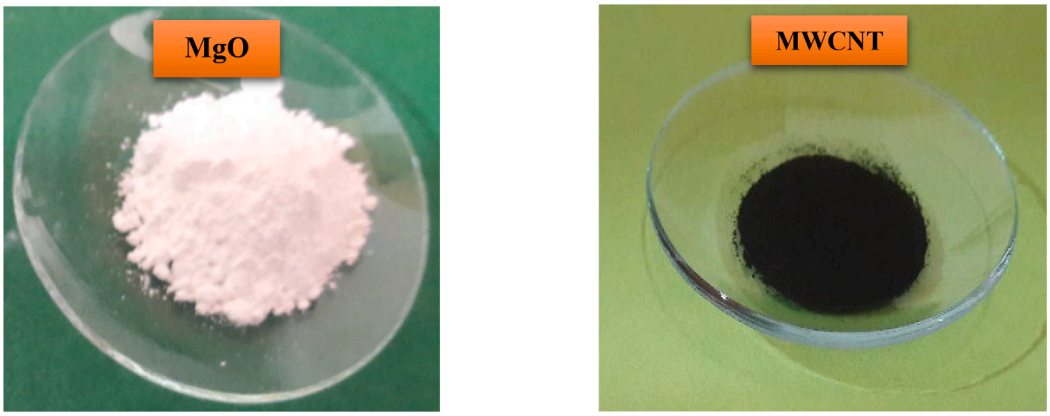

Fig. 3. MgO and MWCNT NPs.

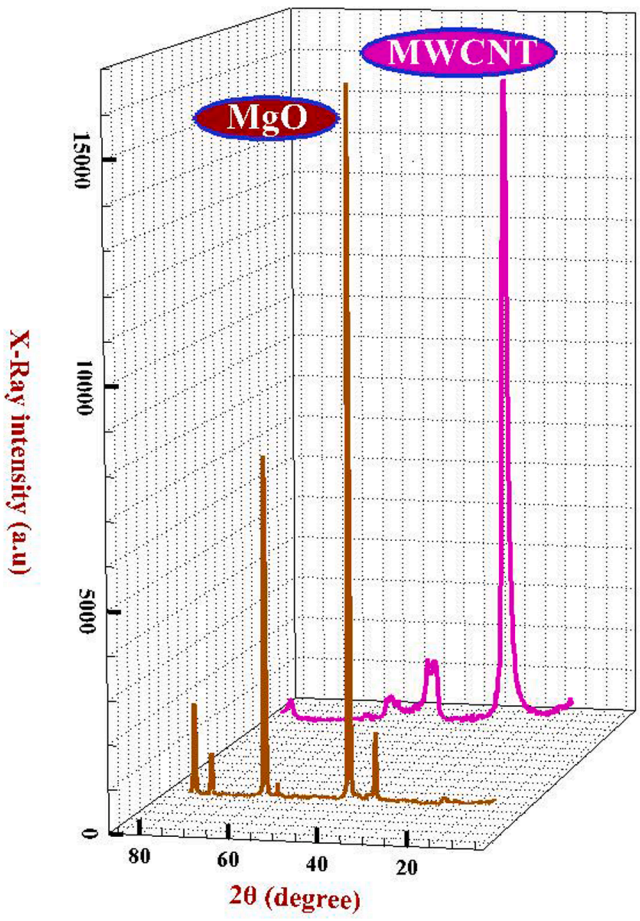

Fig. 4. X-ray diffraction of NPs.

For different volume fractions, The amount of required MWCNT and MgO NPs is and accurately measured using a digital scale determined using Eq. (1) and accurately measured using a digital scale (Fig. 6) with an accuracy of 0.001 gr.

$$\varphi\% = \left(1 - \frac{0.8\left(\frac{w}{\rho}\right)_{MgO}}{0.2\left(\frac{w}{\rho}\right)_{MWCNT} + 0.8\left(\frac{w}{\rho}\right)_{MgO} + \left(\frac{w}{\rho}\right)_{10W40}}\right) \quad (1)$$

By injecting NPs into the BF and preparing the NF, it is necessary to carry out the process of homogenization and uniformity. A magnetic stirrer was used to stabilize NPs in the BF, increase the quality of NFs, and homogenize NFs after the dispersion of the NPs into the BF. (Fig. 7. a). Also, to break the heavy molecules, an ultrasonic vibrator was used for 6 h to create more stability in the suspension and eliminate the agglomeration phenomenon in the NFs. Ultrasonic homogenizer (Ultrasonic homogenizer) is a device for converting electric current into mechanical vibrations, which leads to the homogenization of the ultrasonic system. In the liquid environment, it produces pressure waves and causes a "cavitation phenomenon" under the right conditions. The resulting sound vibration is used to synchronize and destroy the cells (See Fig. 7).

Fig. 8 shows the stabilized NFs at different SVFs such that no precipitation was observed with the naked eye.

2.2. Measurement of dynamic viscosity

Viscosity is the most important fluid characteristic that is used to determine the quality and efficiency of a product. The viscometer in the laboratory will be responsible for an important part of the quick and accurate analysis of a product. Fluids that change their viscosity with their flow need a rheometer to measure the viscosity. Brookfield CAP2000 + viscometer was used to measure viscosity in different laboratory conditions. Working conditions with the viscometer are listed in Table 2. Also, some obtained data from measuring the viscosity of NFs and BF are reported in Table 3. To provide results with less error and more accuracy in rheological behavior, optimization was done. Data extraction is done in two steps. In the first step, before the measurement, the calibration process was performed using the glycerin sample. In the second step, all experiments were measured four times, and then the average data was recorded.

3. Results and discussion

3.1. NF behavior

Fluids are subdivided into Newtonian and non-Newtonian categories

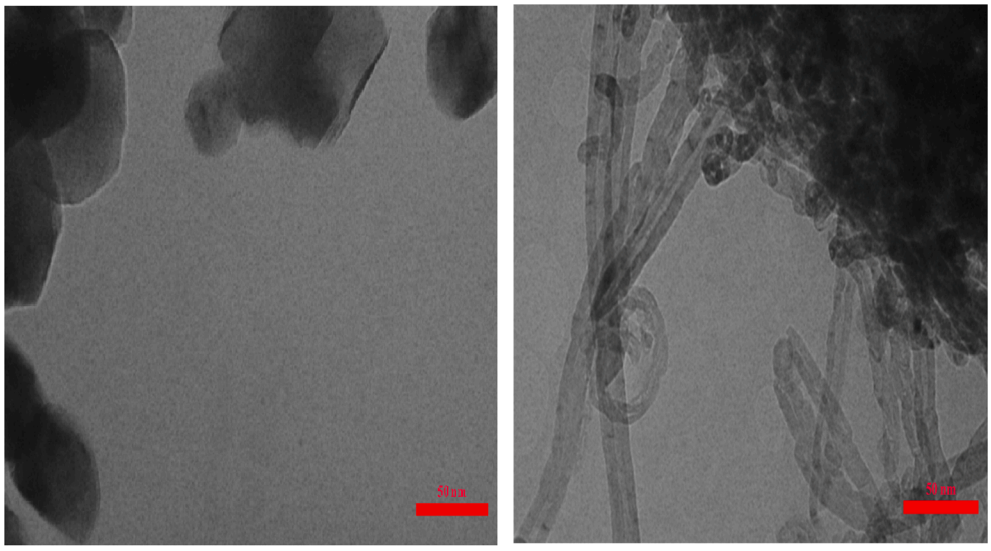

a)MgO b)MWCNT

Fig. 5. TEM of NPs: a) MgO and b) MWCNT.

Fig 6. Digital scale for weighing the NPs.

a) ultrasonic vibration

b) Magnetic stirrer

Fig. 7. Ultrasonic vibration and Magnetic stirrer.

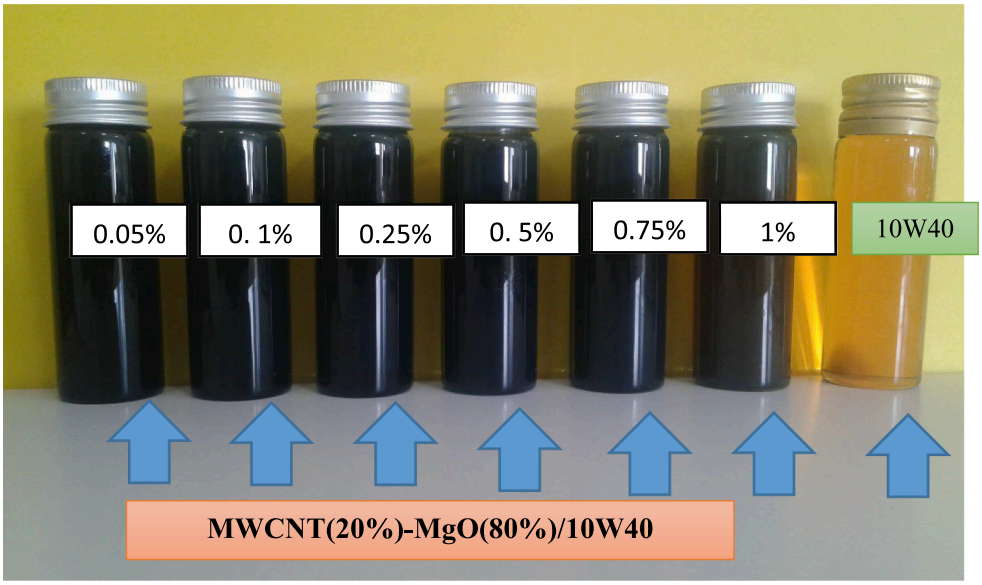

Fig. 8. Prepared NFs.

Table 2
CAP2000 + Viscometer operating conditions.

Descriptions	Specifications
0.2–1500 (pis)	Viscosity
10–13000 (sec^{-1})	SR
130–230 (vac)	Input voltage
50–60 (Hz)	Input frequency
High torque: (dyne.cm)18000–18100	Torque range
Low torque: (dyne.cm)797–7970	
16.3(kg)	Weight
5–75 or 50–233 (°C)	Temperature
RPM)5–1000)	Rate

Table 3
Some data obtained from measuring the viscosity of NFs and BF.

NPs	SVF (%)	T (°C)	SR (s^{-1})	μ(mPa.s)
MWCNT-MgO (20–80 %)/10 W40	0.25	25	2666	170.6
		35	3999	104.4
	0.75	25	3999	182.5
		35	5332	110.6
Oil 10 W40	0	25	3999	142.5
		35	6665	84.4

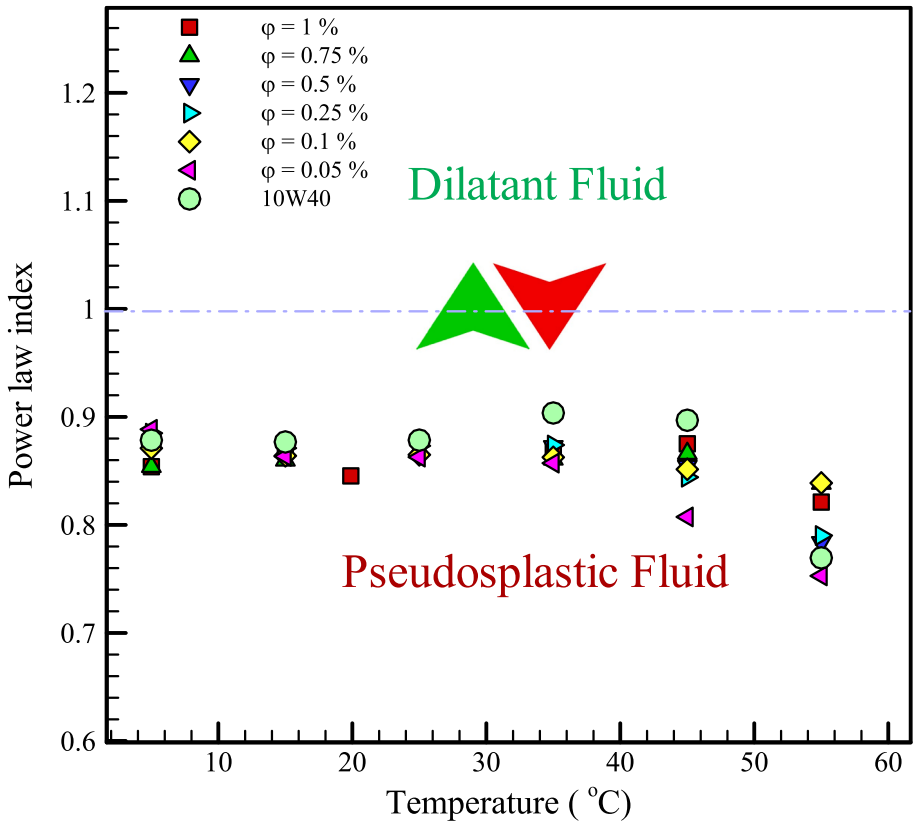

Fig. 9. Power-law index versus svf and temperatures.

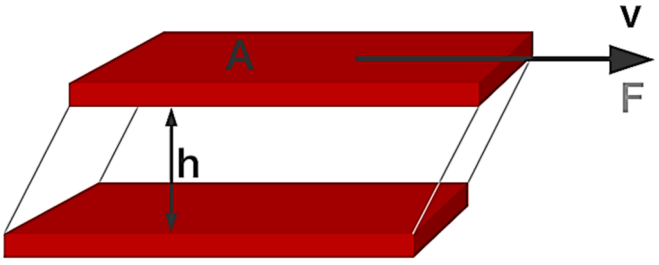

Fig. 10. Layered motion of fluid due to shear force.

depending on their reaction to shear stress. One of these categories is non-Newtonian fluids. In these fluids, the viscosity is a function of shear deformation, and the stress does not change linearly with the SR,

$$\tau = m\dot{\gamma}^n \tag{2}$$

In this respect, n represents the power-law index and m is the consistency index. Fig. 9 shows the power-law index of NFs and oil 10 W40 BF at different SVFs. $n < 1$ at all temperatures and SVFs indicate that all samples are non-Newtonian with shear-thinning behavior.

Viscosity is a measure of the adhesion of a fluid. This adhesion occurs when one surface of the fluid has relative motion relative to the other surfaces, and this adhesion requires a large amount of force to move it which is called 'shear force'. Therefore, using Fig. 10, the viscosity definition is as follows:

$$SR / SS = \text{viscosity}$$

The viscosity of NF at various SRs is presented in Fig. 11. It is shown that increasing temperature has a remarkable effect on reducing viscosity.

3.2. Temperature and solid volume fraction

In most cases, the viscosity depends on the temperature and SVF. As the temperature increases, the intermolecular force decreases and the molecular bonds break down more easily. The viscosity of NF samples decreases with the temperature at SR = 3999 s^{-1} with increasing temperature. As the temperature increases, the interaction between the molecules decreases, and as a result, the viscosity decreases. The dramatic decrease in viscosity due to temperature rise is illustrated in Fig. 12. In general, the viscosity of NF increases with increasing SVF and decreases with increasing temperature.

The percent increase or decrease in the viscosity of NF with SVF is observed in Fig. 13 at SR = 3999 s^{-1} and 6665 s^{-1} and different temperatures and SVFs. The highest increase in viscosity is observed at SR = 3999 s^{-1}, T = 45 °C, and SVF = 0.75 %. In this case, the turbulence between the NPs and the BF is aggravated. Also, at low SVFs, a decrease in viscosity values of up to −5% can be seen.

To illustrate the effect of temperature, SVF, and SR, Fig. 14 is presented. As can be seen, the effect of temperature change had the greatest effect on viscosity. Using this figure can also obtain critical points of

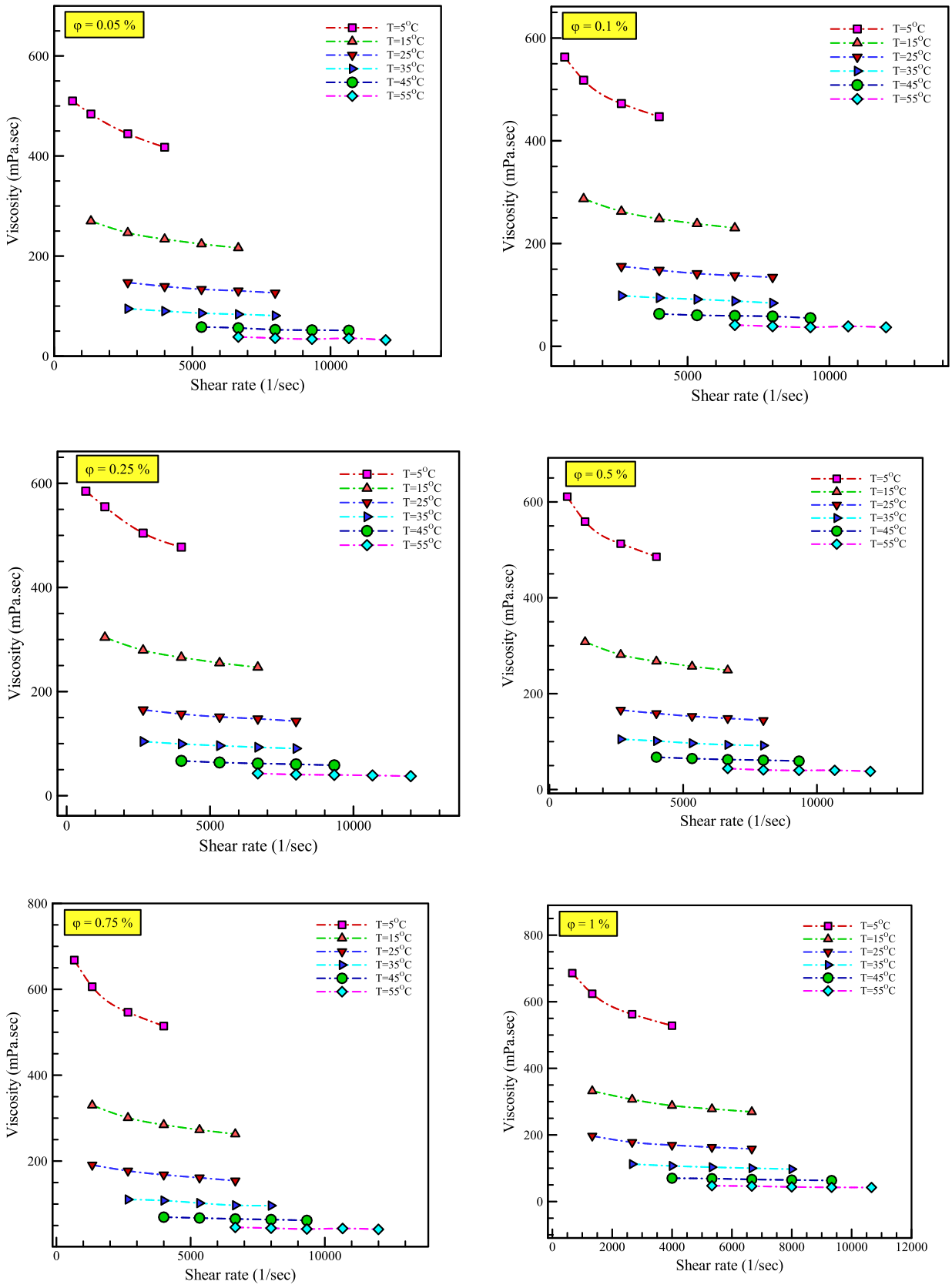

Fig. 11. The viscosity of SR at various temperatures.

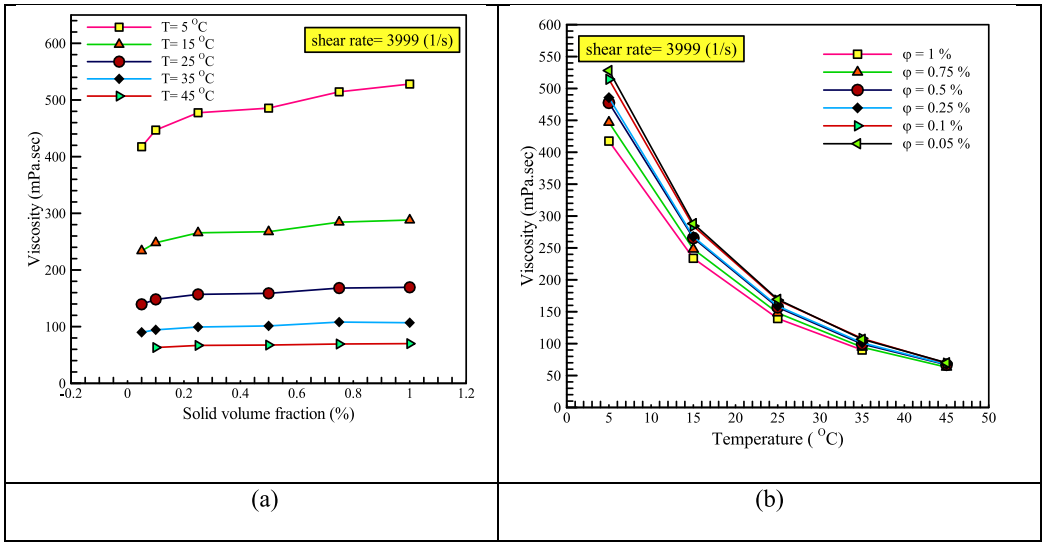

Fig. 12. Viscosity versus temperature at different SVFs (a) SR = 3999 s^{-1} and (b) 6665 s^{-1}.

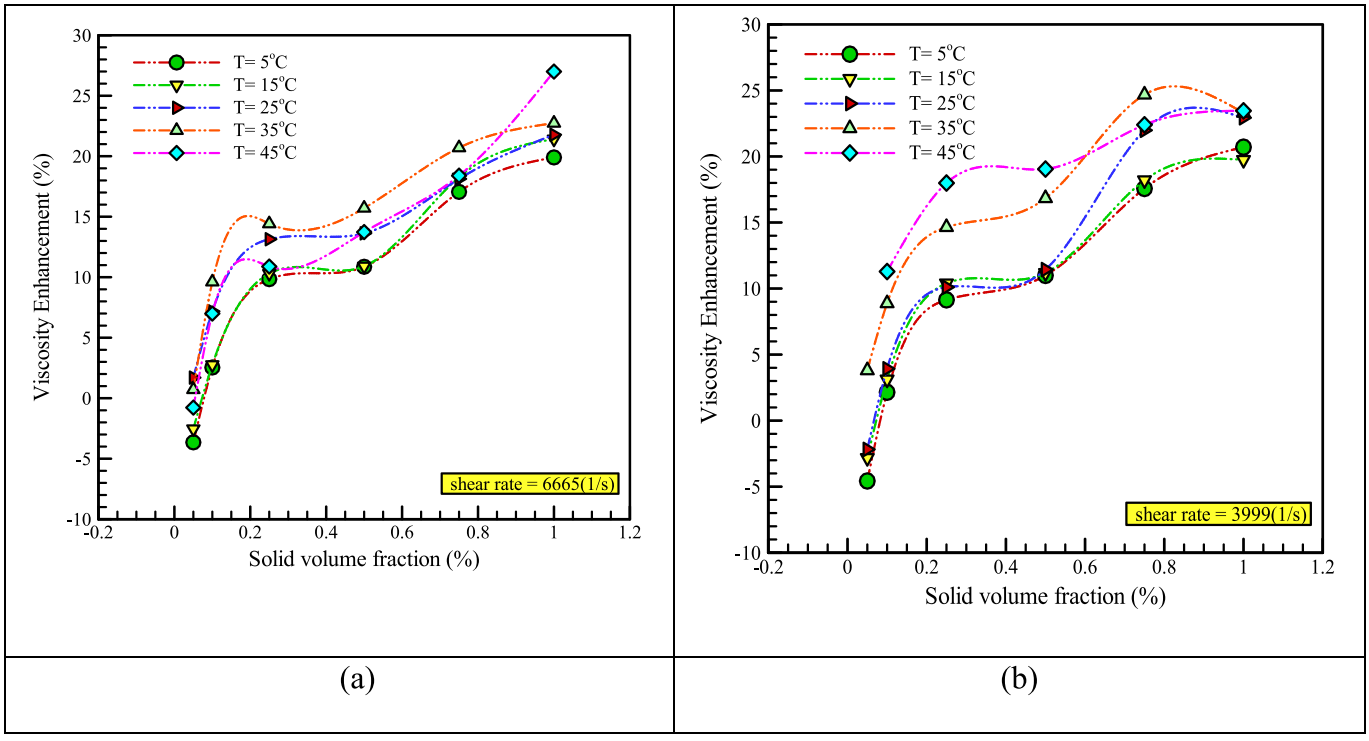

Fig. 13. Viscosity Enhancement of the hybrid NF versus SVF at different temperatures (a) SR = 3999 s^{-1} and (b) 6665 s^{-1}.

response in specified ranges depending on temperature, SVF, and SR.

Also, to investigate the simultaneous effect of two parameters on the viscosity of the mentioned NF, a viscosity curve for temperature and SVF as well as viscosity to temperature and SR is presented in Fig. 15.

3.3. Comparison with other NFs

The presence of NPs in the BFs changes the rheological properties of BFs. One of the properties that change is the viscosity of NF. Viscosity is the most important physical property of fluid when determining lubrication needs. Due to the use of NFs in different systems, increasing or decreasing viscosity can be effective. Increasing viscosity enables the NF to withstand greater capacity and prevents friction therefore increasing the service life of the piece. However, the reduced viscosity reduces the required power for pumping of NFs, which saves energy. The viscosity relative to the SVF at SR = 3999 s^{-1} and T = 15 °C and the viscosity

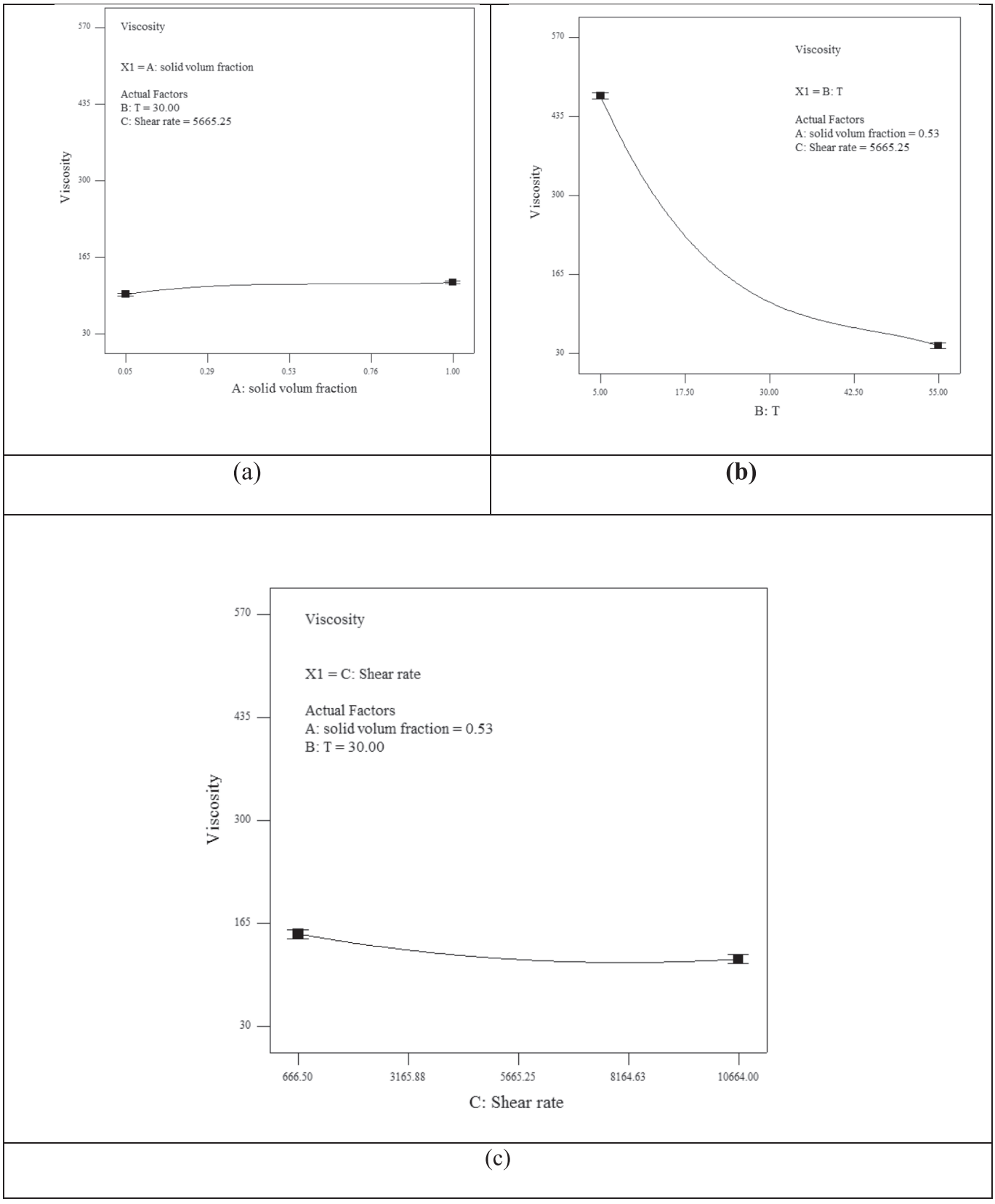

Fig. 14. Effect of (a) SVF, (b) temperature and (c) SR on the viscosity.

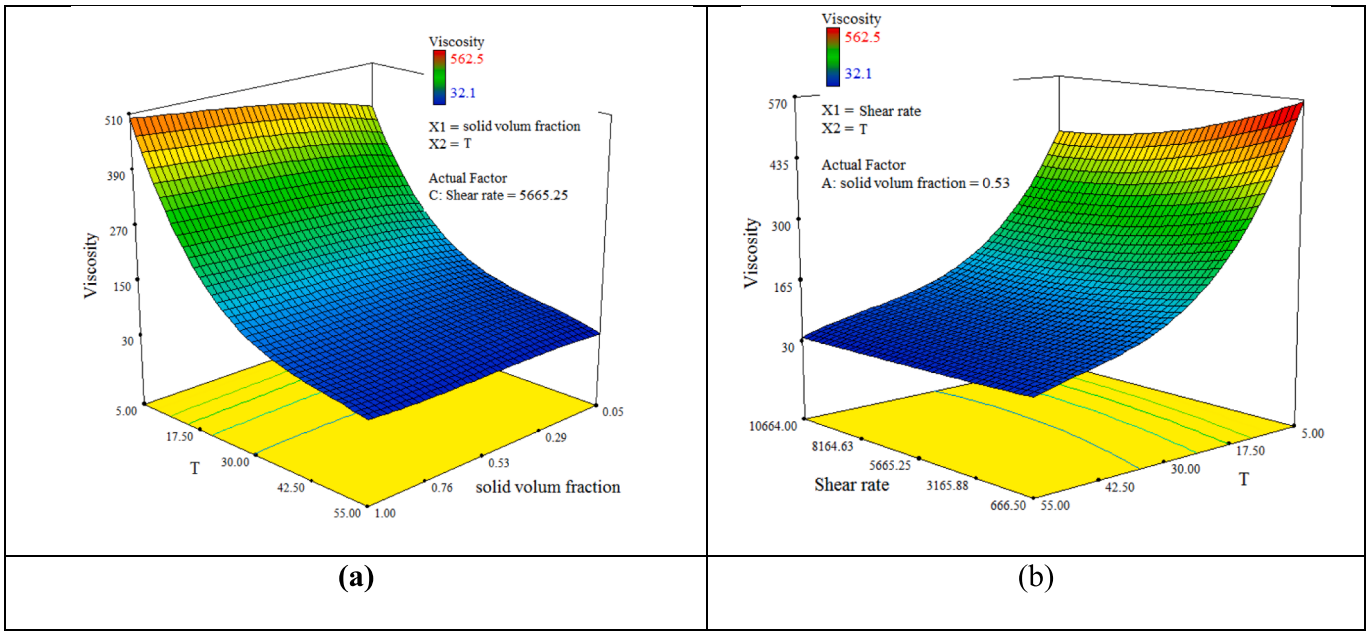

Fig. 15. MWCNT-MgO (20 % –80 %)/10 W40 NF viscosity versus (a) temperature and SVF and (b) temperature and SR.

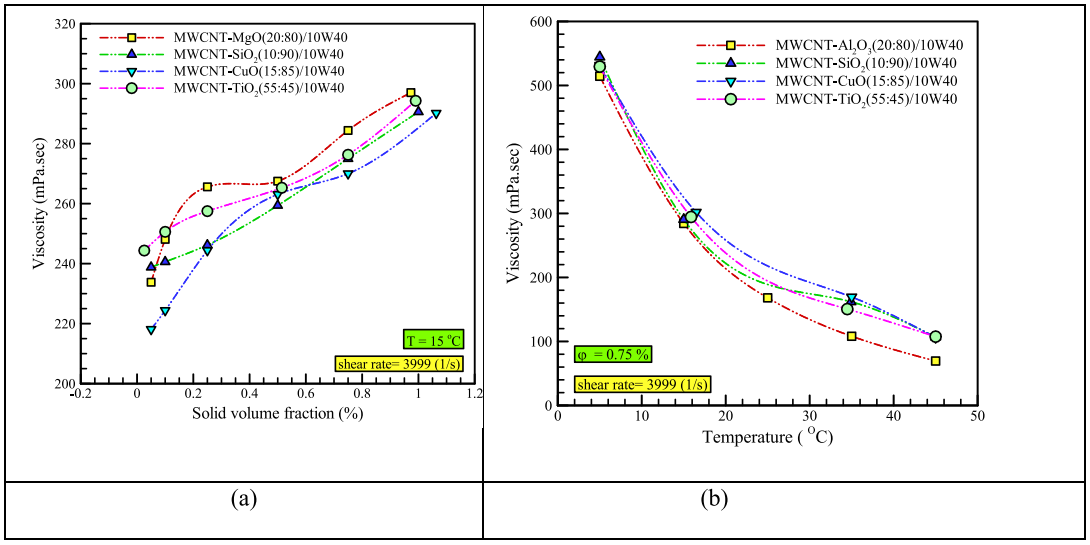

Fig. 16. The viscosity of the various NFs versus (a) SVF and (b) temperature.

relative to the temperature at SVF = 0.75 % is shown in Fig. 16. The experimental data obtained from the MWCNT (20 %)-MgO (80 %)/10 W40 NF with the results of other researches by Hemmat et al. MWCNT (10 %)-SiO_2 (90 %)/10 W40 NF (Nadooshan et al., 2017), MWCNT(15 %)-CuO(85 %)/10 W40 NF (Moghaddam and Motahari, 2017) and MWCNT(55 %)-TiO_2(45 %)/10 W40 NF (Esfe et al., 2021) at different temperatures and SVFs in SR = 3999 s^{-1} were compared. The MWCNT (20 %)-MgO (80 %)/10 W40 NF has the highest viscosity and the MWCNT(15 %)-CuO (85 %)/10 W40 NF has the lowest viscosity due to the different properties of MgO and CuO NPs and their different SVFs, which causes their difference in viscosity.

3.4. Economic assessment

Using an NF can be feasible if the changes made to it are cost-effective. The curve of price performance factor (PPF) versus SVF at T = 15 °C and SR = 3999 s^{-1} to compare MWCNT (20 %) -MgO (80 %) / 10 W40 NF performance with other results by Hemmat et al. (Moghaddam and Motahari, 2017; Esfe et al., 2021; Nadooshan et al., 2017), MWCNT(10–SiO_2(90 %)/10 W40 NF (Nadooshan et al., 2017), MWCNT

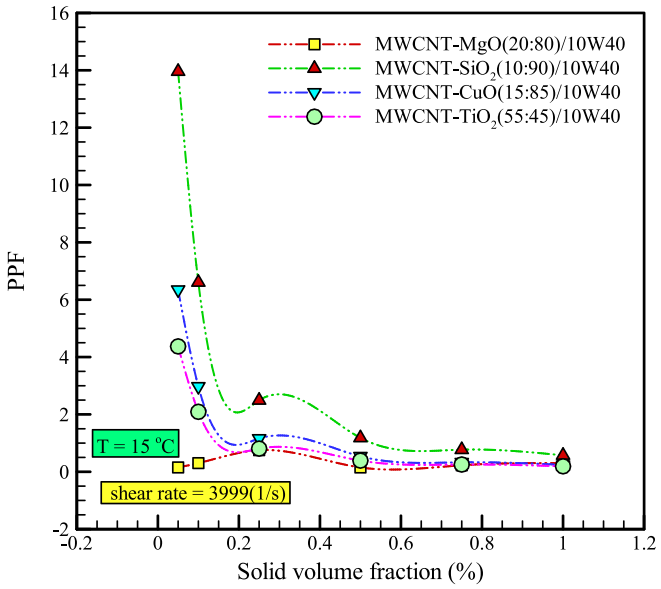

Fig. 17. Comparison of a PPF of the various hybrid NFs.

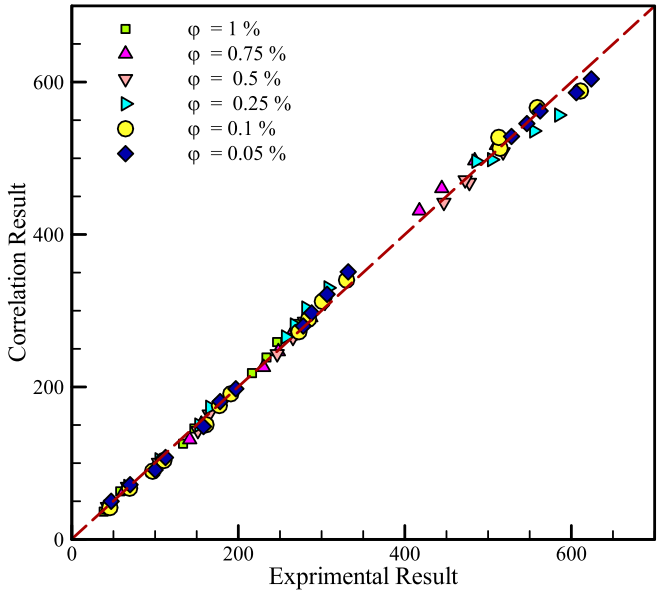

Fig. 18. Conformity of the results.

(15 %)-CuO (85 %)/10 W40 NF (Moghaddam and Motahari, 2017) and MWCNT(55 %)-TiO_2(45 %)/10 W40 NF (Esfe et al., 2021) is shown in Fig. 17. PPF is defined as the ratio of the relative viscosity of the NF to its cost as given in Eq.3:

$$PPF = \frac{RelativeViscosity}{Price(\frac{\$}{lit})} \times 1000 \quad (3)$$

The relative viscosity of one fluid may be greater than that of the other NFs, but its PPF may be lower. As can be seen in Fig. 17, the MWCNT (10 %)-SiO_2 (90 %)/10 W40 NF possesses the best PPF.

3.5. Proposed correlation

To curve-fitting the NF viscosity relation, a stepwise regression method was utilized. In this method, the effect of independent variables on the dependent variable is anticipated well, and the optimal value and portion of each variable are predicted. In the proposed equation (Eq. (4), the viscosity depends on SVF (φ), T, and SR ($\dot{\gamma}$).

$$\begin{aligned}\mu =& 682.23 + 300.40 \times \varphi - 34.61T - 0.03868\dot{\gamma} - 7.10582\varphi T - 0.006 \times \varphi\dot{\gamma} \\ &+ 0.001T\dot{\gamma} - 249.90\varphi^2 + 0.68T^2 + 1.22E-06\dot{\gamma}^2 + 1.70\varphi^2 T \\ &+ 0.060697\varphi T^2 + 4.04E-07\varphi\dot{\gamma}^2 - 1E-07 \times T\dot{\gamma}^2 + 101.8389\varphi^3 \\ &- 0.0054T^3\end{aligned} \quad (4)$$

The matching of the results is shown in Fig. 18. The obtained data are in good agreement which shows the accuracy of the proposed relation. Tables 4 and 5 give the importance of each parameter and the precision Eq.4, respectively. The regression coefficient of the relation is 0.9973 indicating high precision of the offered relation.

The error and MOD curves versus SVF at different temperatures for SR = 6665 s^{-1} are presented in Fig. 19. The results show good agreement.

4. Conclusion

In this study, the rheological behavior of MWCNT-MgO (20 %:80 %)/10 W40 hybrid NF was measured and reported as laboratory analysis with different objectives at T = 5–55 °C at SVF = 0.05 % and 1 %. The main results of this study are classified as follows:

- Changes in temperature and SVF caused changes in the dynamic viscosity of nanofluid in this study. The effects of temperature were greater than volume fraction.
- It was obvious that NFs have non-Newtonian behavior in different temperature conditions and SVFs.
- All NF data show non-Newtonian behavior similar to the shear-thinning model with n < 1.
- The highest frequency of MOD values in different temperatures and SVFs were in the limit of −50 % <MOD<+100 % and it is a sign of very low error of the mathematical relationship of viscosity.
- A new theoretical relationship considering the effect of temperature and SVF parameters is presented to calculate the effective viscosity of NF.
- A stepwise regression method was used to predict the NF viscosity relationship.
- The results of comparing the PPF of different hybrid NFs show that the relative viscosity of this hybrid NF may be higher than other NFs, but its PPF is lower.
- The studied NF will improve the quality and efficiency of the produced engine oil and prevent possible damage to the moving parts of the engine. It reduces the speed and increases the life of the engine, which will be of interest to the craftsmen.

Table 4
Degree of the importance of terms of the proposed model.

Source	Sum of Squares	df	Mean Square	F-Value	p-value Prob > F	
Model	4.016E + 006	16	2.510E + 005	3591.29	< 0.0001	significant
A-SVF	30.96	1	30.96	0.44	0.5067	
B-T	1.063E + 005	1	1.063E + 005	1520.98	< 0.0001	
C-SR	621.10	1	621.10	8.89	0.0033	
AB	7163.45	1	7163.45	102.50	< 0.0001	
AC	50.19	1	50.19	0.72	0.3981	
BC	132.61	1	132.61	1.90	0.1704	
A^2	1860.56	1	1860.56	26.62	< 0.0001	
B^2	1.357E + 005	1	1.357E + 005	1941.92	< 0.0001	
C^2	2427.48	1	2427.48	34.73	< 0.0001	
A^2B	1020.88	1	1020.88	14.61	0.0002	
AB^2	3372.14	1	3372.14	48.25	< 0.0001	
AC^2	174.42	1	174.42	2.50	0.1162	
BC^2	3153.83	1	3153.83	45.13	< 0.0001	
A^3	753.61	1	753.61	10.78	0.0013	
B^3	38511.88	1	38511.88	551.06	< 0.0001	
C^3	460.33	1	460.33	6.59	0.0112	
Residual	10692.67	153	69.89			
Cor Total	4.026E + 006	169				

Table 5
ANOVA for the proposed model.

Std. Dev.	8.36	R^2	0.9973
Mean	173.55	R^2_{adj}	0.9971
C.V. %	4.82	R^2_{pred}	0.9966
PRESS	13627.28	Adeq Precision	217.921

CRediT authorship contribution statement

Mohammad Hemmat Esfe: Methodology,Validation,Investigation, Conceptualization,Data curation.**H. Hatami:** Methodology,Software, Validation,Investigation.**Soheyl Alidoost:** Methodology,Software,Validation,Investigation.**Davood Toghraie:** Methodology,Software,Validation,Writing – original draft,Investigation.

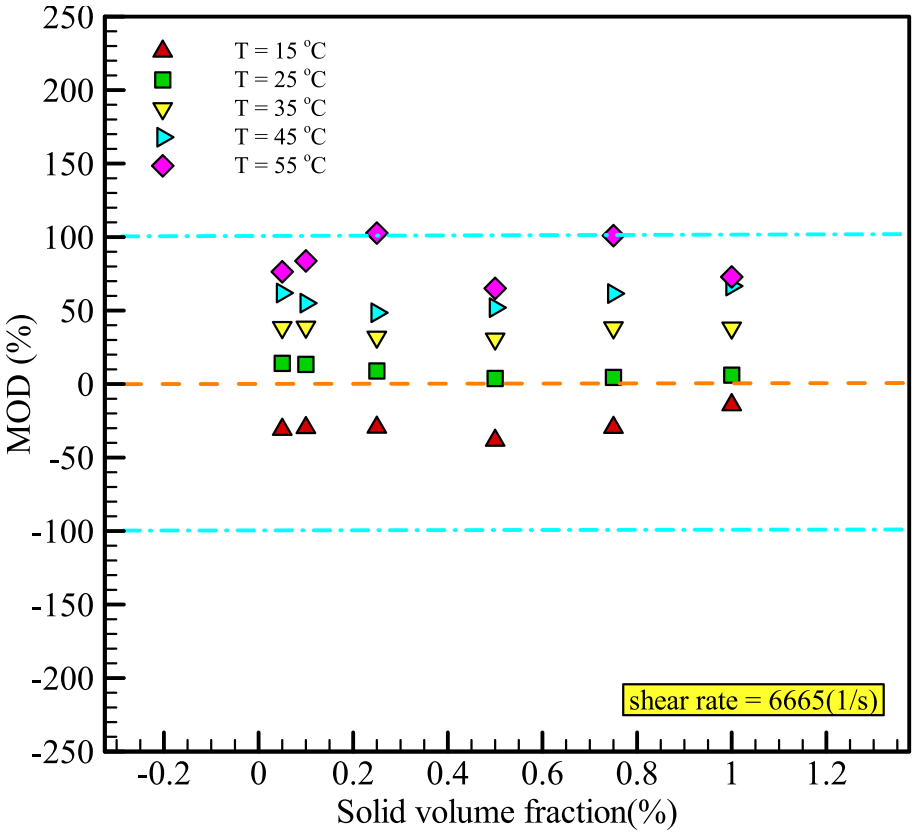

Fig. 19. MOD versus the SVF.

Declaration of Competing Interest

The authors declare that they have no known competing financial interests or personal relationships that could have appeared to influence the work reported in this paper.

References

Abbasian Arani, A.A., Abbaszadeh, M., Ardeshiri, A.J.T.P.N.M.S., 2016. Mixed convection fluid flow and heat transfer and optimal distribution of discrete heat sources location in a cavity filled with nanofluid. *Challenges in Nano and Micro Scale*. Science and Technology 5 (1), 30–43.

Abedian, B., Kachanov, M., 2010. On the effective viscosity of suspensions. Int. J. Eng. Sci. 48 (11), 962–965.

Alidoust, S., AmoozadKhalili, F., Hamedi, S., 2022. Investigation of effective parameters on relative thermal conductivity of SWCNT (15%)-Fe3O4 (85%)/water hybrid ferro-nanofluid and presenting a new correlation with response surface methodology. Colloids Surf A Physicochem Eng Asp 645, 128625.

Alirezaie, A., Saedodin, S., Esfe, M.H., Rostamian, S.H., 2017. Investigation of rheological behavior of MWCNT (COOH-functionalized)/MgO-engine oil hybrid nanofluids and modelling the results with artificial neural networks. J. Mol. Liq. 241, 173–181.

Alizadeh, A., Jasim Mohammed, K., Fadhil Smaisim, G., Hadrawi, S.K., Zekri, H., Taheri Andani, H., Nasajpour-Esfahani, N., Toghraie, D., 2023. Evaluation of the effects of the presence of ZnO -TiO2 (50 %–50 %) on the thermal conductivity of Ethylene Glycol base fluid and its estimation using Artificial Neural Network for industrial and commercial applications. J. Saudi Chem. Soc. 27 (2), 101613 https://doi.org/10.1016/j.jscs.2023.101613.

Banisharif, A., Estellé, P., Rashidi, A., Van Vaerenbergh, S., Aghajani, M., 2021. Heat transfer properties of metal, metal oxides, and carbon water-based nanofluids in the ethanol condensation process. Colloids Surf A Physicochem Eng Asp 622, 126720.

Baratpour, M., et al., 2016. Effects of temperature and concentration on the viscosity of nanofluids made of single-wall carbon nanotubes in ethylene glycol. Int. Commun. Heat Mass Transfer 74, 108–113.

Binu, K.G., Shenoy, B.S., Rao, D.S., Pai, R., 2014. A variable Viscosity Approach for the Evaluation of load Carrying Capacity of oil lubricated Journal Bearing with TiO_2 Nanoparticles as lubricant Additives. Procedia Materials science,6, 1051–1067.

Brinkman, H.C., 1952. The viscosity of concentrated suspensions and solutions. J. Chem. Phys. 20 (4), 571.

Cao, Y., Khan, A., Abdi, A., Ghadiri, M., 2021. Combination of RSM and NSGA-II algorithm for optimization and prediction of thermal conductivity and viscosity of bioglycol/water mixture containing SiO2 nanoparticles. Arab. J. Chem. 14 (7), 103204.

Chen, H., Ding, Y., Tan, C., 2007. Rheological behaviour of nanofluids. New J. Phys. 9 (10), 367.

Dai, X., Andani, H.T., Alizadeh, A., Abed, A.M., Smaisim, G.F., Hadrawi, S.K., Karimi, M., Shamsborhan, M., Toghraie, D., 2023. Using Gaussian Process Regression (GPR) models with the Matérn covariance function to predict the dynamic viscosity and torque of SiO2/Ethylene glycol nanofluid: A machine learning approach. Eng. Appl. Artif. Intel. 122 (106107), 106107 https://doi.org/10.1016/j.engappai.2023.106107.

Dezfulizadeh, A., Aghaei, A., Joshaghani, A.H., Najafizadeh, M.M., 2021. An experimental study on dynamic viscosity and thermal conductivity of water-Cu-SiO2-MWCNT ternary hybrid nanofluid and the development of practical correlations. Powder Technol. 389, 215–234.

Duangthongsuk, W., Wongwises, S., 2009. Measurement of temperature-dependent thermal conductivity and viscosity of TiO 2-water nanofluids. Exp. Therm Fluid Sci. 33 (4), 706–714.

Ehteram, H.R., Abbasian, A.A., Sheikhzadeh, G.A., Aghaei, A., Malihi, A.R., 2016. The effect of various conductivity and viscosity models considering Brownian motion on nano fluids mixed convection flow and heat transfer.

Einstein, A., 1906. Eine neue bestimmung der moleküldimensionen. Ann. Phys. 324 (2), 289–306.

Esfe, M.H., Sarlak, M.R., 2017. Experimental investigation of switchable behavior of CuO-MWCNT (85%–15%)/10W-40 hybrid nano-lubricants for applications in internal combustion engines. J. Mol. Liq. 242, 326–335.

Esfe, M.H., Arani, A.A.A., Rezaie, M., Yan, W.M., Karimipour, A., 2015. Experimental determination of thermal conductivity and dynamic viscosity of Ag–MgO/water hybrid nanofluid. Int. Commun. Heat Mass Transfer 66, 189–195.

Esfe, M.H., Rostamian, H., Sarlak, M.R., Rejvani, M., Alirezaie, A., 2017. Rheological behavior characteristics of TiO2-MWCNT/10w40 hybrid nano-oil affected by temperature, concentration and shear rate: an experimental study and a neural network simulating. Physica E 94, 231–240.

Esfe, M.H., Esfandeh, S., Toghraie, D., 2021. Feasibility study of using MWCNT-TiO2 (25: 75) in 5W50 as an optimizer for engine oils with the aim of reduce the cold start damages. Int. Commun. Heat Mass Transfer 129, 105678.

Eshaghi, A., Mojab, M., 2017. Hydrophilicity of Silica Nano-Porous Thin Films: Calc fects of multi-walled carbon nanotubes on rheological behavior of engine ination Temperature Effects. J. Nanostruct. 7 (2), 127–133.

Frankel, N.A., Acrivos, A., 1967. On the viscosity of a concentrated suspension of solid spheres. Chem. Eng. Sci. 22 (6), 847–853.

Fuxi, S., Hamedi, S., Hajian, M., Toghraie, D., Alizadeh, A.A., Hekmatifar, M., Sina, N., 2021. Addition of MWCNT-Al2O3 nanopowders to water-ethylene glycol (EG) base fluid for enhancing the thermal characteristics: Design an optimum feed-forward neural network. Case Studies. Therm. Eng. 101293.

Ghanbari, M., Rezazadeh, G., 2021. A MEMS-based methodology for measurement of effective density and viscosity of nanofluids. European Journal of Mechanics-B/fluids 86, 67–77.

Godson, L., et al., 2010. Experimental investigation on the thermal conductivity and viscosity of silver-deionized water nanofluid. Experimental Heat Transfer23.4 317–332.

Guzman. K.A.D., Taylor. M.R., Banfield. J.F. (2006). Environmental risks of nanotechnology: national nanotechnology initiative funding, 2000–2004. Environ. Sci. Technol. 40.; 1401–1407.

Hemmat Esfe, M., Saedodin, S., Wongwises, S., Toghraie, D., 2015. An experimental study on the effect of diameter on thermal conductivity and dynamic viscosity of Fe/water nanofluids. J. Therm. Anal. Calorim. 119, 1817–1824.

Hosseini, S. M. S., & Dehaj, M. S. (2021). Assessment of TiO2 water-based nanofluids with two distinct morphologies in a U type evacuated tube solar collector. Applied Thermal Engineering, 182, 116086.

Hosseini, S.M.S., Dehaj, M.S., 2021. An experimental study on energetic performance evaluation of a parabolic trough solar collector operating with Al2O3/water and GO/water nanofluids. Energy 234, 121317.

Hosseinian Naeini, A., Baghbani Arani, J., Narooei, A., Aghayari, R., Maddah, H., 2016. Nanofluid thermal conductivity prediction model based on artificial neural network. Challenges in Nano and Micro Scale Science and Technology 4 (2), 41–46.

Jamei, M., Olumegbon, I.A., Karbasi, M., Ahmadianfar, I., Asadi, A., Mosharaf-Dehkordi, M., 2021. On the Thermal Conductivity Assessment of Oil-Based Hybrid Nanofluids using Extended Kalman Filter integrated with feed-forward neural network. Int. J. Heat Mass Transf. 172, 121159.

Keykhosravi, A., Vanani, M.B., Aghayari, C., 2021. TiO_2 nanoparticle-induced Xanthan Gum Polymer for EOR: Assessing the underlying mechanisms in oil-wet carbonates. J. Pet. Sci. Eng. 204, 108756.

Krieger, I.M., Dougherty, T.J., 1959. A mechanism for non-Newtonian flow in suspensions of rigid spheres. Transactions of the Society of Rheology 3 (1), 137–152.

Makinde, O.D., Mishra, S.R., 2017. On stagnation point flow of variable viscosity nanofluids past a stretching surface with radiative heat. International Journal of Applied and Computational Mathematics 3 (2), 561–578.

Moghaddam, M.A., Motahari, K., 2017. Experimental investigation, sensitivity analysis and modeling of rheological behavior of MWCNT-CuO (30–70)/SAE40 hybrid nano-lubricant. Appl. Therm. Eng. 123, 1419–1433.

Mooney, M., 1951. The viscosity of a concentrated suspension of spherical particles. J. Colloid Sci. 6 (2), 162–170.

Mousavi, S.M., Ehteshami, B., Darzi, A.A.R., 2021. Two-and-three-dimensional analysis of Joule and viscous heating effects on MHD nanofluid forced convection in microchannels. Thermal Science and Engineering Progress 25, 100983.

Mousavi, S.B., Heris, S.Z., Estellé, P., 2021. Viscosity, tribological and physicochemical features of ZnO and MoS2 diesel oil-based nanofluids: An experimental study. Fuel 293, 120481.

Nadooshan, A.A., Esfe, M.H., Afrand, M., 2017. Evaluation of rheological behavior of 10W40 lubricant containing hybrid nano-material by measuring dynamic viscosity. Physica E 92, 47–54.

Raei, B., Shahraki, F., Jamialahmadi, M., Peyghambarzadeh, S.M., 2016. Experimental investigation on the heat transfer performance and pressure drop characteristics of γ-Al2O3/water nanofluid in a double tube counter flow heat exchanger. Challenges in Nano and Micro Scale Science and Technology 5 (1), 64–75.

Ruhani, B., Andani, M.T., Abed, A.M., Sina, N., Smaisim, G.F., Hadrawi, S.K., Toghraie, D., 2022. Statistical modeling and investigation of thermal characteristics of a new nanofluid containing cerium oxide powder. Heliyon 8 (11), e11373.

Saboori, R., Sabbaghi, S., Barahoei, M., Sahooli, M., 2017. Improvement of thermal conductivity properties of drilling fluid by CuO nanofluid. Challenges in Nano and Micro Scale Science and Technology 5 (2), 97–101.

Shahsavar, A., Jamei, M., Karbasi, M., 2021. Experimental evaluation and development of predictive models for rheological behavior of aqueous Fe3O4 ferrofluid in the presence of an external magnetic field by introducing a novel grid optimization based-Kernel ridge regression supported by sensitivity analysis. Powder Technol.

Sun, Y.L., Toghraie, D., Akbari, O.A., Pourfattah, F., Alizadeh, A.A., Ghajari, N., Aghajani, M., 2021. Thermal performance and entropy generation for nanofluid jet injection on a ribbed microchannel with oscillating heat flux: Investigation of the first and second laws of thermodynamics. Chin. J. Chem. Eng.

Tian, S., Arshad, N.I., Toghraie, D., Eftekhari, S.A., Hekmatifar, M., 2021. Using perceptron feed-forward Artificial Neural Network (ANN) for predicting the thermal conductivity of graphene oxide-Al2O3/water-ethylene glycol hybrid nanofluid. Case Studies in Thermal Engineering 26, 101055.

Tseng, W.J., Chen, C.-N., 2003. Effect of polymeric dispersant on rheological behavior of nickel–terpineol suspensions. Mater. Sci. Eng. A 347 (1), 145–153.

Valantina, S.R., Jayalatha, K.A., Angeline, D.P., Uma, S., Ashvanth, B., 2018. Synthesis and characterisation of electro-rheological property of novel eco-friendly rice bran oil and nanofluid. J. Mol. Liq. 256, 256–266.

Wangjian, H.E.N.G., Yunlong, Z.H.A.N.G., Lilong, G.A.O., et al., 2021. Research on Rheological Properties and Constitutive Equation of GHL Explosive. Journal of Ordnance Equipment. Engineering 42 (10), 103–108.

Wu, X., Li, C., Zhou, Z., Nie, X., Chen, Y., Zhang, Y., Sharma, S., 2021. Circulating purification of cutting fluid: an overview. The International Journal of Advanced Manufacturing Technology 117 (9–10), 2565–2600.

Yang, X., Boroomandpour, A., Wen, S., Toghraie, D., Soltani, F., 2021. Applying Artificial Neural Networks (ANNs) for prediction of the thermal characteristics of water/

ethylene glycol-based mono, binary and ternary nanofluids containing MWCNTs, titania, and zinc oxide. Powder Technol. 388, 418–424.
Yu, H., Duan, B., Feng, L., Kalbasi, R., 2021. Thermophysical properties improvement of a common liquid by adding reduced graphene oxide: An experimental study. Powder Technol. 384, 466–478.
Zhang, Z., Yang, F., Zhang, H., Zhang, T., Wang, H., Xu, Y., et al., 2021. Influence of CeO2 addition on forming quality and microstructure of TiCx-reinforced CrTi4-based laser cladding composite coating. Materials Characterization, 171. doi: 10.1016/j.matchar.2020.110732.